JOURNAL OF MATERIALS SCIENCE 15 (1980) 1140–1146

Creep deformation of V_3Si single crystals

D. M. NGHIEP, P. PAUFLER*, U. KRÄMER, K. KLEINSTÜCK
Technische Universität Dresden, Sektion Physik, 8027 Dresden, Mommsenstrasse 13, DDR

N. H. QUYEN
Zentralinstitut für Festkörperphysik und Werkstofforschung, Dresden der Akademie der Wissenschaften der DDR, 8027 Dresden, Helmholtzstrasse 20, DDR

From the experiments during steady state creep of V_3Si single crystals at $T = 1280$ to 1400° C and $\sigma = 1$ to 7×10^7 Pa, activation volumes, 10 to 70 b^3, and activation enthalpies, 2 to 11 eV, have been derived. With deviation from stoichiometric composition a hardening effect has been experimentally established. It is suggested that the rate controlling process was due to dislocation glide and dynamic recovery by dislocation climb.

1. Introduction

The intermetallic compound V_3Si (A-15 or Cr_3Si type structure) is of primary interest from the viewpoint of superconductivity. Levinstein *et al.* [1] succeeded in demonstrating the ductility of a thick wafer of V_3Si single crystal at 1520° C by an indentation technique. Recently, Mahajan *et al.* [2] reported the dynamic deformation of V_3Si at temperatures between 1200 and 1800° C. A systematic investigation of macroscopic deformation in V_3Si has been carried out since 1975 under dynamic [3, 4] and static [5–8] conditions at temperatures of 1040 to 1700° C. As a part of these studies, the main results of secondary creep deformation associated with TEM observations in V_3Si single crystals will be presented in the present paper.

2. Experimental procedure

The creep deformation was realized in an improved compression apparatus in a vacuum of 130×10^{-5} Pa described elsewhere [6, 8, 9]. Temperatures (T) and applied stresses (σ) varied between 1280 and 1400° C and 1×10^7 and 7×10^7 Pa, respectively. The specimen was situated between two compression pieces of a tungsten alloy. The specimen heating was performed in a tantalum resistance furnace. The absolute error of temperature measurement amounted to max ± 8 K. The accuracy of stress determination was better than 10 %.

The V_3Si single crystals used were grown by a zone melt technique with electron beam heating (cf. [10]). The real structure of grown crystals was reported by Paufler *et al.* [11]. The samples were spark machined from cylindrical rods and the processing was carried out using machine grinding, machine polishing and/or electropolishing. The second phase was identified by means of metallographic analysis [3, 12] (see Table I). The samples were middle oriented and suitable for compression.

The influence of plastic deformation upon superconducting properties was reported by Quyen *et al.* [13]. The average composition of each sample was determined by a combined measurement of resistance ratio r and lattice parameter, as described elsewhere [10, 11]. To reveal the real structure, the specimens were prepared for etch pitting and TEM study before and after deformation. To determine the activation parameters, either load change (LC) or temperature change (TC) tests were performed. The experimental parameters are given in Table I.

3. Results and discussion

3.1. General information

Deformation proceeded inhomogeneously. This agrees with the results obtained by surface marking

*Present address: Karl-Marx-Universität Leipzig, 703 Leipzig, Scharnhorststraße 20, DDR.

 0022–2461/80/051140–07$02.70/0

TABLE I Experimental characteristics

Specimen no.	Dimension		T_c (K)	r_{20}^{-1}K	Treatment	Metallogr.	Experiment	T (° C)	σ (10^7 Pa)	ϵ (%)
	$\bar{l}_0$ (10^{-3} m)	$\bar{F}_0$ (10^{-5} m^2)								
115 Z2/L2.1	7.88	1.29	16.79	37.50	SC, MG, MP, E	SCr, SP	LC	1350–1450	1.5–4.2	32
115 Z2/L2.2	7.56	1.22	16.79	37.50	SC, MG, MP, E, TEM	SCr, SP	LC	1340–1380	1.3–3.5	13
117 Z2/L2.2	7.51	0.97	16.87	58.21	SC, MG, MP, TEM	SCr, SP	LC	1370–1420	1.0–4.0	21
119 Z2/L2.1	7.61	1.33	16.70	21.42	SC, MG, MP, E	SCr, SP	TC	1400–1310	1.5	9
								1290–1400	2.2	
119 Z2/L2.2	6.77	1.42	16.66	23.69	SC, MG, MP, EP, E	SCr, SP	TC	1390–1280	1.3	4
85 Z2/L5.2	8.52	1.16	16.84	20.41	SC, MG, MP, E, TEM	SCr, SP	LC	1280–1400	1.7–8.5	16
							TC	1400–1280	3.8	
85 Z2/L5.4	9.75	1.28	16.65	47.51	SC, MG, MP, E	SCr, SP	LC	1400–1280	1.2–4.9	9
							TC	1280–1400	2.7	
75 Z2/L3.6.2	7.24	1.11	16.85	8.50	SC, MG, MP, E	SCr, ∝V	LC	1280–1400	0.8–5.2	7
							TC	1400–1280	3.1	
V62–M16	8.58	1.17	16.65	18.59	SC, MG, MP, EP, E	SCr, V_5Si_3	LC	1280–1400	1.2–5.4	35
V60–M15.1							TC	1400–1280	2.9	
V62–M16	8.72	1.50	16.50	17.50	SC, MG, MP, E	SCr, V_5Si_3	LC	1280–1400	1.2–5.5	12
V60–M15.2							TC	1400–1280	2.9	
M21 Z2/L2.5	8.99	0.97	16.74	28.27	SC, MG, MP, E	SCr, SP	LC	1280–1390	1.0–5.6	19
M21 Z2/L2.7	7.48	1.57	16.67	40.62	SC, MG, MP, E	SCr, SP	TC	1400–1280	3.1	27
							LC	1280–1380	1.3–5.3	
127 Z2/L2.5	8.22	1.18	16.77	33.64	SC, MG, MP, E, EP	SCr, V_5Si_3	LC	1280–1400	1.6–6.2	19
129/130 Z2/L2.8	7.58	1.33	16.87	13.85	SC, MG, MP, E	SCr, SP	LC	1280–1400	1.5–5.9	17
134 Z2/L2.2	8.14	1.08	16.87	25.58	SC, MG, MP, E	SCr, SP	LC	1280–1410	1.8–7.2	29
134 Z2/L2.3	8.10	1.09	16.87	25.71	SC, MG, MP, E	GB, SP	LC	1280–1400	1.8–7.2	23
134 Z2/L2.4	8.20	1.23	16.88	25.35	SC, MG, MP, E, TEM	GB, SP	TC	1280–1400	2.4, 3.2	15
								1400–1280	4, 4.8, 5.6	
134 Z2/L2.5	8.07	1.45	16.80	43.14	SC, MG, MP, E	GB, V_5Si_3	LC	1280–1400	1.7–5.1	20
							TC	1400–1280	3.7	
134 Z2/L2.6	8.07	1.55	16.80	14.75	SC, MG, MP, E	GB, V_5Si_3	LC	1280–1400	1.3–6.0	18
							TC	1400–1280	4.4	
135 Z2/L3.1	9.29	1.02	16.80	42.21	SC, MG, MP, E, TEM	SCr, SP	LC	1280–1400	1.0–5.8	27
							TC	1400–1280	2.9	
135 Z2/L3.4	8.00	0.90	16.72	23.76	SC, MG, MP, E	GB, SP	TC	1400–1280	3.2	21
							LC	1280–1400	1.1–4.3	
135 Z2/L3.5	7.86	1.05	16.74	35.40	SC, MG, MP, E	SCr, SP	LC	1280–1400	0.9–5.1	26
							TC	1400–1280	2.8	
135 Z2/L3.6	8.12	1.17	16.74	31.97	SC, MG, MP, E	SCr, SP	LC	1280–1400	0.8–5.0	28
							TC	1400–1280	2.5	
135 Z2/L3.7	7.66	1.13	16.72	16.20	SC, MG, MP, E	SCr, SP	TC	1400–1280	2.6	33
							LC	1400–1280	0.9–5.6	
135 Z2/L3.8	7.87	1.04	16.80	13.67	SC, MG, MP, E	SCr, V_5Si_3	TC	1400–1280	2.8	11
							LC	1400–1280	0.9–5.2	

Notes: $\bar{l}_0$ mean length, $\bar{F}_0$ mean cross-section, T_c critical temperature, $R_{20\,K}$ resistance at 20 K, $R_{293\,K}$ resistance at 293 K, T specimen temperature, σ applied stress, ϵ deformation, SC spark cutting, MG machine grinding, MP machine polishing, EP electropolishing, TEM transmission electron microscopy, E etching, SP single phase, SCr single crystal, GB grain boundary, TC temperature change, LC load change.

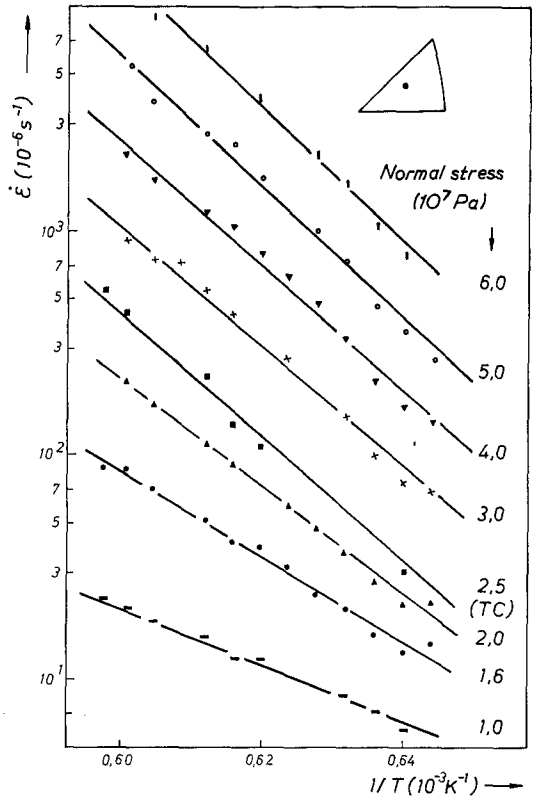

Figure 1 The influence of temperature (T) on the steady state creep rate ($\dot{\varepsilon}$) in V_3Si. Specimen I35 Z2/L3.6.

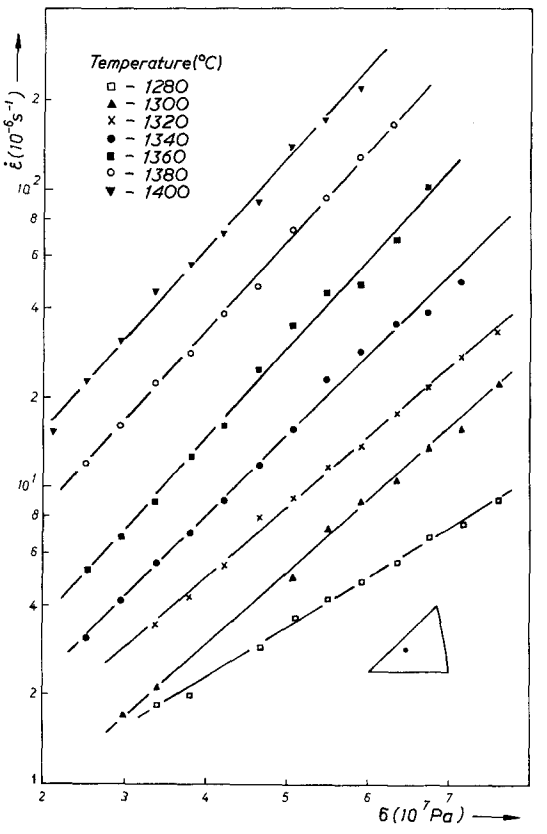

Figure 2 Stress dependence of steady creep rate ($\dot{\varepsilon}$) of V_3Si. Load change experiment. Specimen 85 Z2/L5.2.

[6], asterism analysis and TEM observations [14]. The inhomogeneity of deformation may be due to inhomogeneous temperature distribution, friction [15], fluctuation of chemical composition and fluctuation of the grown-in dislocation density. Slip lines could not be resolved since a surface layer had formed during high temperature deformation.

Registered creep curves showed two distinct creep stages. The transition creep is alternated gradually by steady state creep with increasing temperature. At temperatures $\geqslant 1350^\circ$ C and stresses $\sigma \geqslant 2$ to 3×10^7 Pa, the secondary creep stage starts immediately after loading.

3.2. Temperature

Steady state creep rate ($\dot{\varepsilon}$) has been found to depend strongly on temperature. The results are shown in Fig. 1 at different applied stresses for a single-phase crystal. The data were obtained by load change experiments. The temperature dependence of $\dot{\varepsilon}$ can be described by an exponential function $\exp(-\Delta H_{exp}/kT)$, where ΔH_{exp} is an apparent activation enthalpy. This behaviour agrees with that of the Laves phase $MgZn_2$ [16–19].

3.3. Stress

The effect of stress on creep rate may be seen in Fig. 1. If $\ln \dot{\varepsilon}$ is plotted against σ, a linearity is observed for specimens on the vanadium-rich side (Fig. 2).

3.4. Activation parameters

Activation parameters were obtained by means of activation analysis [20, 21]. The apparent activation volumes (V_{exp}) are (10 to 70)b^3 (b is Burgers vector), i.e. lie between the results for bcc and hcp metals [22]. Activation volumes increase with increasing temperature and decreasing stress (for excess Si). On the silicon-rich side, V_{exp} is larger than on the other side (Fig. 4). The V_{exp} (and ΔH_{exp}) variation with stress may be due to a change in the rate controlling process. The effect of composition can be related to different types of point defects existing on both sides of stoichiometry [11, 13] and their interaction with dislocations.

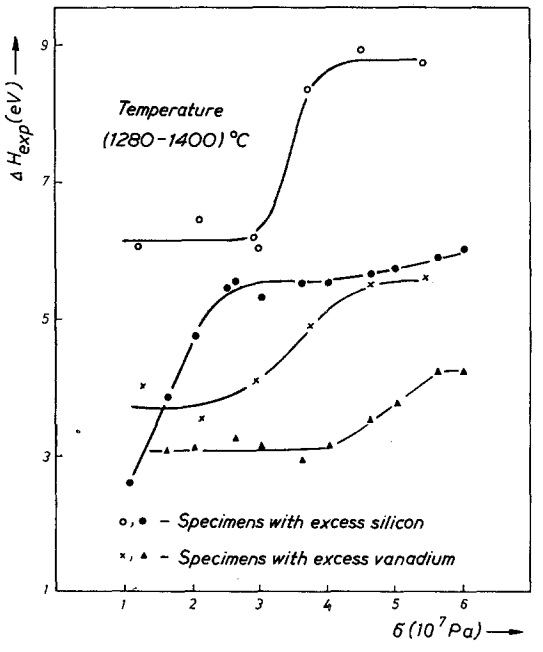

Figure 3 Activation enthalpy (ΔH_{exp}) as a function of the normal stress (σ) for V_3Si.

Apparent activation enthalpies were found to be relatively large (2 to 11 eV) (cf. [23]) and dependent on applied stress and composition (Fig. 3 and 4). The figures of ΔH_{exp} compare with those for poly-phase structures (e.g. 8.24 and 9.54 eV for TD–Ni and Fe–Mo–Mo_2C, respectively [21]) and would be expected for a compound like V_3Si with a high melting point T_m (1935° C) [24]. Direct observation of dislocations after deformation by TEM showed regular networks of small-angle boundaries (cf. Section 3.6). The activation enthalpy found in V_3Si single crystals should be attributed to glide and climb processes of dislocations during dynamic recovery. As mentioned above, the activation enthalpy increases in a step-like manner with applied stress. The ΔH_{exp} curve consists of one or two plateau regions with a change occurring over a small stress range (Fig. 3). The anomalous stress dependence can be caused by the stress effect on the arrangement of alternative obstacles [20].

3.5. Composition

In Fig. 4, steady state creep rate and activation parameters are plotted versus resistance ratios ($r_{20\,K} = R_{20\,K}/R_{293\,K}$) used as a measure for the chemical compositions of V_3Si. For non-stoichiometric crystals, a hardening effect was found, i.e. the steady state creep rate decreases towards both sides of stoichiometric composition. A similar effect was observed with hardness [3, 9] and flow stress [4], in accordance with the observation of creep rate. Many elements and solid solutions [25, 31] have been found to behave in this way. On the other hand, a solid solution softening has been observed in solid solutions, ionic crystals [21, 25] and intermetallic compounds [26–29]. Following Westbrook [30], these behaviours are interpreted in terms of the misordering inevitably introduced by point defects with deviation from stoichiometry. The increase in ΔH_{exp} towards the vanadium and silicon sides (Fig. 4) means that thermally activated motion of dislocations becomes more difficult for off-stoichiometric compositions. The results of density [11], resistance and superconducting parameters [13] suggest a dominating role of point defects during deformation.

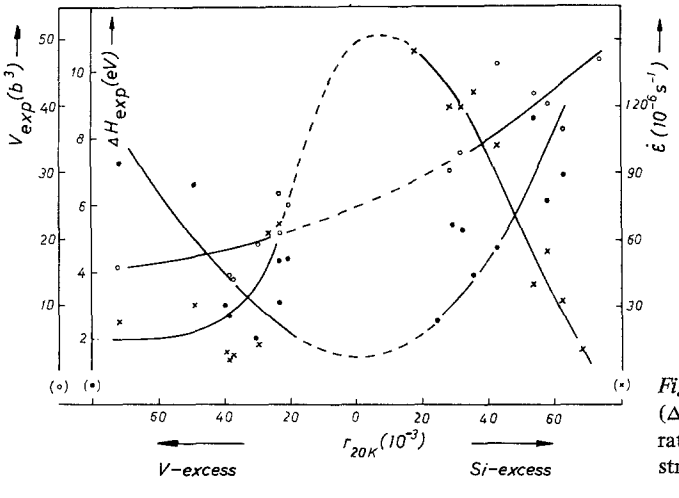

Figure 4 Steady state creep rate ($\dot{\varepsilon}$), activation enthal (ΔH_{exp}) and activation volume (V_{exp}) versus resistan ratio (r_{20K}) of V_3Si. Temperature $T = 1400°$ C. Norn stress $\sigma = 3 \times 10^7$ Pa.

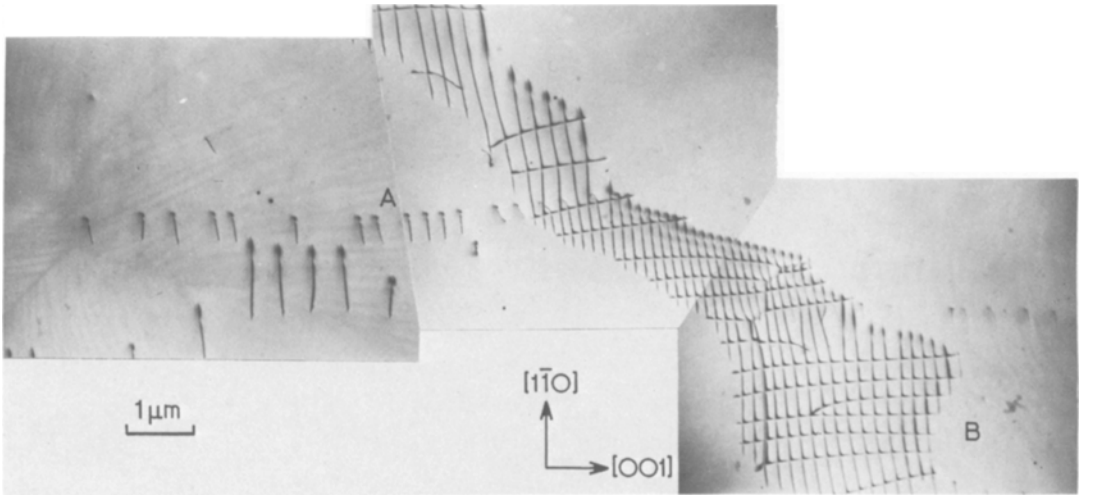

Figure 5 Subgrain boundaries in a creep deformed V_3Si single crystal ($\epsilon = 32\%$, $T = 1450°$ C, $\sigma = 4.2 \times 10^7$ Pa). TEM foil normal $\approx$ [1 1 0], acceleration voltage 200 kV.

3.6. TEM observations

All the samples investigated by TEM were deformed several times by TC and/or LC tests. In the following figures, ϵ is the total strain reached after the tests, T is the temperature and σ the stress at the last test.

The transparent regions always show many subgrain boundaries. Their density is significantly increased in comparison with that of undeformed crystals [11]. In some TEM specimens, very regularly formed subgrain boundaries with grains nearly free of dislocations have been observed (Fig. 5). Obviously the recovery is very advanced. The glide dislocations have arranged themselves by climb processes in an energetically favourable manner. The so-formed subgrains are inclined one with another by some minutes of arc. Using the invisibility criterion ($\mathbf{g} \cdot \boldsymbol{b} = 0$) the Burgers vectors were determined. According to this, the subgrain boundaries are formed by two sets of dislocations with Burgers vectors of the type $\boldsymbol{b} = \langle 1\,0\,0 \rangle$. This type was always found with glide dislocations [32–34]. From the arrangement of dislocations it may be concluded that the tilt axes of the subgrains are of the type $\langle 1\,0\,0 \rangle$ [35]. This result was confirmed by X-ray Laue diagrams.

In Fig. 5 the boundary A is a tilt boundary on the plane (0 1 0). Parallel edge dislocations along the [1 0 0] direction are observed with a Burgers vector [0 1 0] and a tilt axis [1 0 0]. Tilt boundaries of this kind are the most frequent type

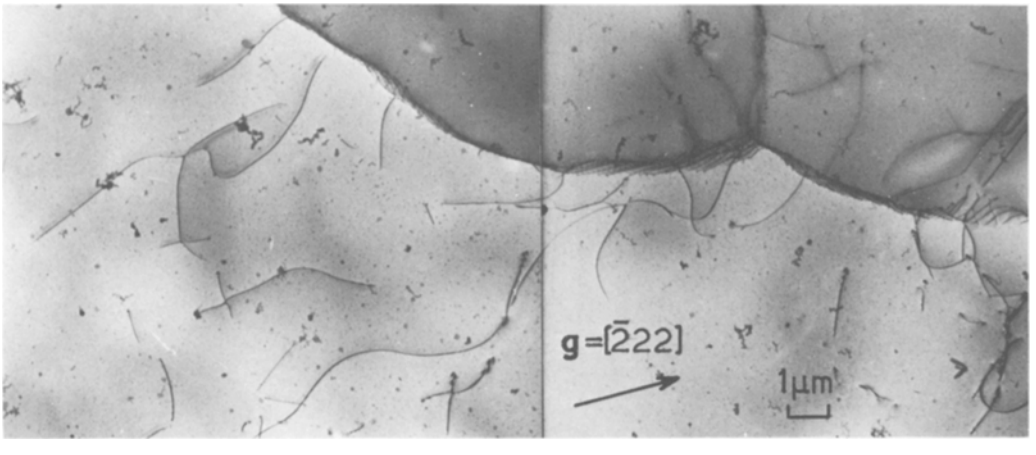

Figure 6 Subgrain boundaries and glide dislocations in a creep deformed V_3Si single crystal ($\epsilon = 16\%$, $T = 1280°$ C, $\sigma = 3.8 \times 10^7$ Pa). TEM foil normal [1 1 0], acceleration voltage 200 kV.

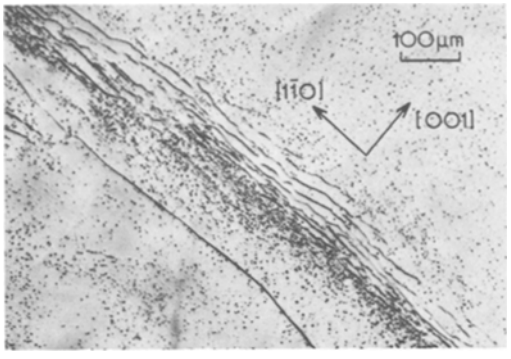

Figure 7 Distribution of dislocations after creep deformation of V_3Si as revealed by etching on a (1 1 0) plane (for details of the etching procedure see [36]).

of subgrain boundaries. On the other planes, dislocations with $\boldsymbol{b} = [0\,0\,1]$ take part, for instance on the plane (1 1 0) in the region B, screw dislocations with this Burgers vector are seen. In another TEM specimen, with the same orientation, grains with the tilt axis [0 0 1] were found. There were almost only tilt boundaries. The distance between them was some microns, and the dimension in the [0 0 1] direction some tens of microns. The subgrains end in twist boundaries on the plane (0 0 1), built up by two orthogonal sets of screw dislocations, or on planes with higher indexes.

In other specimens we found less recovered regions (Fig. 6). The subgrains contain glide dislocations. Their curvature may be due to blocking by Cottrell clouds*. Many of these glide dislocations end in subgrain boundaries, which obviously are sources or sinks for dislocations. In all cases dislocations with different Burgers vectors were found, thus multiple slip must have been taken place.

According to the investigation of other crystals, the degree of recovery does not depend on T or σ. On the other hand, etch pits on a large surface show regions with a very distinct degree of recovery in the same sample (Fig. 7).

4. Conclusions

The intermetallic compound V_3Si may be plastically deformed at constant load at temperatures above $\approx 1280^\circ$ C. Compressional creep rates of the order of $\approx 10^{-6}$ sec^{-1} are obtained at normal stresses of ≈ 10 MPa.

A strengthening effect has been found with deviation from the stoichiometric composition.

On a microscopic scale, the plastic deformation under the conditions investigated is governed by dislocation glide and recovery processes.

Acknowledgements

The authors are grateful to Dr M. Jurisch and Mr J. Behr for supply of V_3Si single crystals. They wish to thank Dr S. Däbritz for his lattice constant measurements, Dr K. Eichler and Mr A. San Martin for many helpful discussions during the experimental work. In addition, the authors would like to express their thanks to all members of the Metal and X-ray Physics Group of the Technische Universität Dresden for their help and support of this work.

References

1. H. J. LEVINSTEIN, E. S. GREINER and H. MASON Jr, *J. Appl. Phys.* 37 (1966) 164.
2. S. MAHAJAN, J. H. WERNICK. G. Y. CHIN, S. NAKAHARA and T. H. GEBALLE, *Appl. Phys. Letters* 33 (1978) 972.
3. B. SCHILD, Diploma work, Sektion Physik, Technische Universität Dresden, (1980).
4. M. BERTRAM, Thesis, Technische Universität Dresden (1980).
5. K. KESSLER, Diploma work, Technische Universität Dresden, (1980).
6. G. BÖHME, Diploma work, Technische Universität Dresden, (1980).
7. A. SAN MARTIN, Thesis, Technische Universität Dresden (1980).
8. D. M. NGHIEP, Thesis, Technische Universität Dresden (1980).
9. "Realstruktureinfluß auf ausgewählte Eigenschaften von Supraleitern des Cr_3Si-Typs", Sektion Physik, Technische Universität Dresden (1978).
10. M. JURISCH, K.-H. BERTHEL and H. J. ULLRICH, *Phys. Stat. Sol. (a)* 44 (1977) 277.
11. P. PAUFLER, E. ZEDLER, H.-J. ULLRICH, K.-H. BERTHEL, U. KRÄMER, M. JURISCH, K. RICHTER and K. EICHLER, *ibid* 44 (1977) 499.
12. "Metallographische Charakterisierung von V_3Si-Schmelzprodukten", Zentralinstitut für Festkörperphysik und Wekstofforschung Dresden der AdW der DDR (1974).
13. N. H. QUYEN, P. PAUFLER, K.-H. BERTHEL, M. BERTRAM, U. KRÄMER, D. M. NGHIEP, A. SAN MARTIN, A. GLADUN and K. KLEINSTUCK, *Phys. Stat. Sol. (a)* 56 (1979) 231.
14. T. KÖHLER, Diploma work, Sektion Physik, Technische Universität Dresden (1978).
15. P. PAUFLER, Thesis, Technische Universität Dresden (1967).
16. K. EICHLER, Thesis, Technische Universität Dresden (1973).
17. S. SIEGEL, Thesis, Technische Universität Dresden (1973).
18. P. PAUFLER and G. E. R. SCHULZE, in "Neuere

*According to recent investigations the curvature of the dislocations is caused by their climbing out of the glide planes.

Entwicklung der Physik" edited by P. Görlich, A. Eckardt and P. Kunze (VEB Deutscher Verlag der Wissenschaft, Berlin, 1974) p. 162.
19. D. HINZ, P. PAUFLER and G. E. R. SCHULZE, *Phys. Stat. Sol.* **36** (1969) 609.
20. U. P. KOCKS, A. S. ARGON and M. F. ASHBY, Thermodynamics and Kinetics of Slip, in "Progress in Materials Science" (Pergamon Press, New York, 1975) sections 25, 43, 44.
21. B. ILSCHNER, "Hochtemperatur-Plastizität" (Springer-Verlag, Berlin. 1973) p. 162.
22. A. G. EVANS and R. D. RAWLINGS, *Phys. Stat. Sol.* **34** (1969) 9.
23. G. E. R. SCHULZE and P. PAUFLER, "Die plastische Verformung 'spröder' intermetallischer Verbindungen und ihre Elementarprozesse" (Akademie-Verlag, Berlin, 1972, Mathematischnaturwissenschaftlische Klasse, Band 51, Heft 5).
24. JU. A. KOČERŽINSKIJ, O. G. KULIK and E. A. SHISHKIN, *DAN SSSR* **209** (1973) 1347.
25. O. D. SHERBY and P. M. BURKE, Mechanical Behaviour of Crystalline Solids at Elevated Temperature, in "Progress in Materials Science" Vol. 13, no. 7 (Pergamon Press, London, 1967).
26. K. EICHLER, S. SIEGEL, H. KUBSCH and P. PAUFLER, *Wiss. Z. Technische Universität Dresden* **20** (1970) 950.
27. P. PAUFLER, K. EICHLER and G. E. R. SCHULZE, *Monatsber. Dtsch. Akad. Wiss. Berlin* **12** (1970) 950.
28. D. L. WOOD and J. H. WESTBROOK, *Trans. Met. Soc. AIME* **224** (1962) 1024.
29. M. I. KORNILOW and N. M. MATVEYEVA, *DAN SSSR* **146** (1962) 642.
30. J. H. WESTBROOK, *Met. Trans.* 8A (1977) 1327.
31. P. HAASEN, in "Physical Metallurgy", edited by R. W. Cahn (North Holland, Amsterdam, 1970) p. 1011.
32. U. ESSMANN, H. HAAG and G. G. ZERWECK, *Commun. Phys.* **2** (1977) 127.
33. U. KRÄMER, K. EICHLER and CH. REINHOLD, 9th Conference "Elektronenmikroskopie", Dresden, Tagungsband, (1978) p. 185.
34. A. BEN LAMINE, F. REYNAUD, C. MAI and I. P. SENATEUR, *Phil. Mag.* **A38** (1978) 359.
35. K. KLEINSTÜCK, U. KRÄMER, P. PAUFLER and H. -J. ULLRICH, *Wiss. Z. Technische Universität Dresden* **29** (1980) 77.
36. A. I. GOHAR, K. KLEINSTÜCK, U. KRÄMER and P. PAUFLER, *Crystal Technol.* **15** (1980) to be published.

Received 3 August and accepted 20 September 1979.